Discovery of Tyrosine Kinase Inhibitors by Docking into an Inactive Kinase Conformation Generated by Molecular Dynamics

Hongtao Zhao, Danzhi Huang,* and Amedeo Caflisch*[a]

Several small molecules that bind to the inactive DFG-out conformation of tyrosine kinases (called type II inhibitors) have shown a good selectivity profile over other kinase targets. To obtain a set of DFG-out structures, we performed an explicit solvent molecular dynamics (MD) simulation of the complex of the catalytic domain of a tyrosine kinase receptor, ephrin type-A receptor 3 (EphA3), and a manually docked type II inhibitor. Automatic docking of four previously reported type II inhibitors was used to select a single snapshot from the MD trajectory for virtual screening. High-throughput docking of a pharmacophore-tailored library of 175 000 molecules resulted in about 4 million poses, which were further filtered by van der Waals efficiency and ranked according to a force-field-based energy function. Notably, around 20 % of the compounds with predicted binding energy smaller than -10 kcal mol^{-1} are known type II inhibitors. Moreover, a series of 5-(piperazine-1-yl)isoquinoline derivatives was identified as a novel class of low-micromolar inhibitors of EphA3 and unphosphorylated Abelson tyrosine kinase (Abl1). The in silico predicted binding mode of the new inhibitors suggested a similar affinity to the gatekeeper mutant T315I of Abl1, which was verified in vitro by using a competition binding assay. Additional evidence for the type II binding mode was obtained by two 300 ns MD simulations of the complex between N-(3-chloro-4-(difluoromethoxy)-phenyl)-2-(4-(8-nitroisoquinolin-5-yl)piperazin-1-yl)acetamide and EphA3.

Introduction

Protein kinases represent attractive targets in oncology drug discovery.[1] One such target is Abelson tyrosine kinase (Abl1), for which small-molecule drugs are employed in the clinics to treat chronic myelogenous leukemia (CML). However all current drugs including imatinib, nilotinib and dasatinib are incapable of inhibiting the most notable T315I gatekeeper mutant, detected in 10–20 % of patients with CML after failure of imatinib therapy.[2,3] Another interesting class of targets is the erythropoietin-producing human hepatocellular carcinoma receptors (Eph), the largest family of receptor tyrosine kinases. The Eph receptors have been implicated in sprouting angiogenesis and blood vessel remodeling during vascular development.[4–7] Furthermore, overexpression of several of the 14 known Eph receptors, including ephrin type-A receptor 3 (EphA3), has been linked to tumors and the associated vasculature, suggesting a critical role in tumor-related angiogenesis.

The majority of small-molecule kinase inhibitors developed so far target the ATP binding site of the kinase in its active state (DFG-in), and are known as type I inhibitors.[8] However, the first kinase-targeting small molecule to reach the market was imatinib (Gleevec), a type II tyrosine kinase inhibitor that binds to the inactive state of Abl1 characterized by a closed conformation of the activation loop (DFG-out). The flip of the DFG motif, a conserved triad (Asp–Phe–Gly) at the beginning of the activation loop, induces remarkable changes in the ATP binding site and exposes an additional hydrophobic pocket that is less conserved in sequence.[9] Many kinase inhibitors have failed in preclinical or clinical development due to their lack of selectivity causing intolerable side effects, largely because the kinase ATP binding site is highly conserved in sequence and conformation.[10] The emergence of type II inhibitors creates new opportunities by targeting the allosteric pocket of the DFG-out conformation, offering selectivity and intellectual property novelty.[11]

Structure-based virtual screening of type II inhibitors requires experimentally available DFG-out protein structures, which were initially limited in availability. As a result, most known type II inhibitors to date have been developed via quantitative structure–activity relationship (QSAR)-guided modifications of ATP binding site ligands.[8] Several computational approaches have been proposed to convert a kinase from a DFG-in into a DFG-out conformation, such as DOLPHIN by deleting about six residues of the activation loop starting with the DFG motif.[12] More recently, a protein remodeling program has been used to model a DFG-out conformation by using the DFG-in as a template structure.[13] At present, a few pharmaceutically relevant kinases have been co-crystallized with type II inhibitors. Even so, literature reports describing the discovery of type II inhibitors by virtual screening remain rare. One reason for this is an induced fit in the protein X-ray structure in favor of the co-crystallized inhibitor; if the biased bind-

[a] H. Zhao, Dr. D. Huang, Prof. A. Caflisch
Department of Biochemistry, University of Zurich
Winterthurerstrasse 190, 8057 Zurich (Switzerland)
E-mail: dhuang@bioc.uzh.ch
caflisch@bioc.uzh.ch

ing site of a single X-ray structure is used, poor docking results are common when using structurally diversified ligands. The unfavorable interactions, particularly clashes between putative ligands and the kinase, on the other hand, would be accommodated by the rearrangement of the protein target, due to the plasticity of the loops around the ATP binding site. The failure of docking diversified ligands thus calls for a generalized binding site in structure-based virtual screening, in order to explore a larger chemical space. The discovery of type II inhibitors is further complicated in that such inhibitors target a relatively scarcely populated protein conformation,[14] which is presumably kinase dependent.[15]

Here, we report the identification of type II inhibitors by flexible ligand docking into an EphA3 structure generated by molecular dynamics (MD). We first run a constrained MD simulation with explicit solvent to induce a fit of the EphA3 structure to a known type II inhibitor that could not be docked into the original X-ray structure. In silico screening was then carried out by pharmacophore filtering, high-throughput docking, and ranking based on an energy function with continuum solvation and hydrogen bonding penalty. Retrospectively, we identify ten classes of known type II scaffolds, none of which could be discovered based on the original X-ray structure and among which some are reported to be active against EphA3. Prospectively, our endeavors lead to the identification of a novel class of low micromolar type II inhibitors, which retains inhibitory activity against the T315I gatekeeper mutant of Abl1.

Figure 1. Previously reported type II inhibitors of EphA3.[16,17] The values next to the compound number are the experimentally measured dissociation constant against phosphorylated EphA3 and the predicted binding free energy. The latter was calculated using the MD-IF structure and a scoring function with continuum solvation and hydrogen bonding penalty.[21]

1
240 nM; −10.2 kcal mol^{-1}

2
3500 nM; −10.2 kcal mol^{-1}

3
1900 nM; −10.3 kcal mol^{-1}

4
80 nM; −9.8 kcal mol^{-1}
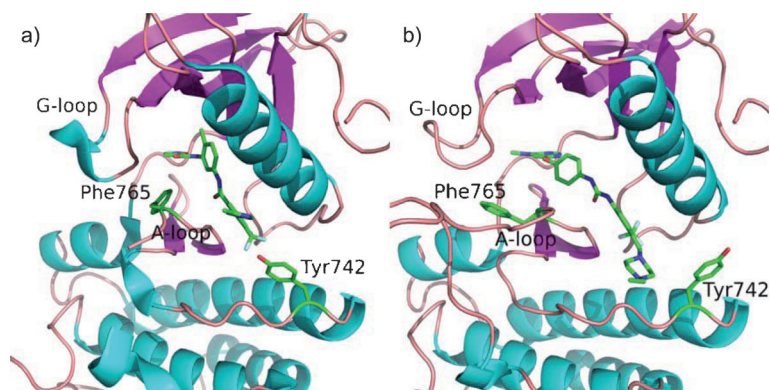
Figure 2. Comparison of a) the crystal structure (PDB: 3DZQ) of the complex of EphA3 with inhibitor **1** and b) the binding mode obtained by docking compound **4** into the MD-IF structure. The comparison shows the different orientations of Tyr 742 and Phe 765, and the difference in the G-loop.

Results and Discussion

Inducing a generalized DFG-out conformation by MD

Induced fit in favor of a specific inhibitor exists in the X-ray crystal structure of EphA3 co-crystallized with compound **1** (PDB: 3DZQ),[16] as none of compounds **2** to **4**[17] (Figure 1) can be docked into the X-ray structure in a type II binding mode without clashes. Specifically, the glycine-rich loop (G-loop), which can adopt various conformations,[10] collapses into the ATP binding site and tightly encompasses the small type I head group of compound **1**. As a consequence, the bigger type I head groups of compounds **2** to **4** in the ATP binding site would clash with the G-loop. In addition, the side chain of Tyr 742 blocks the entry of the piperazine group of compound **4** (Figure 2a). Experimentally, different orientations of the Tyr 742 side chain have been reported in the X-ray structures

of DFG-in EphA3 (PDB: 2QOB[18]) and EphA4 (PDB: 2Y6O and 2Y6M[19]). Computationally, we have observed that the Tyr 742 side chain can adopt two distinct, equally populated orientations in the DFG-out conformation based on ten 50 ns explicit solvent MD simulations of EphA3 (PDB: 3DZQ) with a trifluoromethylbenzene in the allosteric site (Figure S1 in the Supporting Information). These MD simulations were carried out using the protocols described in our previous work,[20] and a detailed analysis of these results will be presented elsewhere.

In the present work, the χ_1 angle of the side chain of Tyr 742 was rotated from −173° (as in 3DZQ) to −60°, and compound **1** was manually replaced by compound **2** to obtain a generalized binding site that can accommodate diversified ligands. Explicit solvent MD with harmonic constraints on all C$_\alpha$ atoms ex-

cluding the G- and A-loops was then carried out for 2 ns. The first 1 ns segment of the trajectory was discarded, and seven snapshots in the second half of the trajectory were selected as they preserve the five intermolecular hydrogen bonds shown in Figure 3. These seven snapshots were minimized over 200
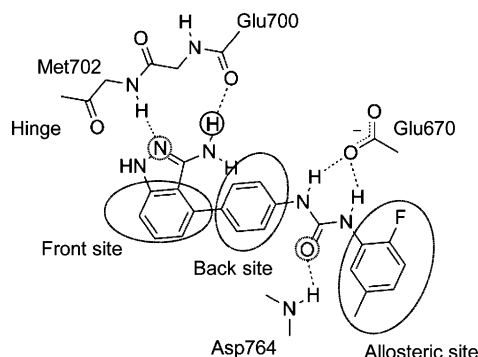
Figure 3. Pharmacophore mapping of the key interactions of type II kinase inhibitors illustrated by compound **2** and EphA3. Hydrogen bonds are shown as dashed lines. Pharmacophore elements used to filter the ZINC library: two acceptors (dashed circles), one donor (solid circle), and three hydrophobic rings (ovals). The hydrogen bond to Glu670 was not used as a pharmacophore because of the flexibility and solvent exposure of the Glu670 side chain (see text for discussion). Details of the geometric constraints are illustrated in Figure S2 in the Supporting Information.

steps, and then compound **2** together with all water molecules were removed. Flexible docking of compounds **1–4** into each of the seven structures was further used to select a single structure for screening according to the binding affinity, which was estimated by a previously reported scoring function using exactly the same parameters.[21] The selected snapshot is called the molecular dynamics induced fit (MD-IF) structure. It should be pointed out that the induced displacements of the G- and A-loops and reorientation of Tyr742 are not achievable by simple energy minimization.

Pharmacophore tailoring the ZINC library

The majority of kinase inhibitors—including type II inhibitors—are hinge binders. They usually form a key hydrogen bond with the backbone NH of the hinge, which belongs to Met702 in the case of EphA3. A hydrogen bond with the carbonyl oxygen of Glu700 is also observed, including the acidic CH groups as donors.[21] For type II inhibitors, an additional pair of hydrogen bonds can be observed with Asp764 of the DFG motif, and the catalytically important Glu670 from the αC-helix (Figure 3).[8] However, the hydrogen bond with Glu670 is surrounded by water molecules, and this hydrogen bond is kinetically not stable.[22] Aside from the hydrogen-bonding interactions, most type II inhibitors can be mapped well into three major hydrophobic interactions: ATP front site, ATP back site, and the allosteric site (Figure 3). The combination of three hydrogen bonds with three hydrophobic groups and their relative separations used as constraints (Figure S2 in the Supporting Information) reduces the 9 millions compounds in the ZINC

library (August 2011) to less than 200 000 molecules (Figure 4) within 6 h on a single Xeon 2.8 GHz central processing unit (CPU).
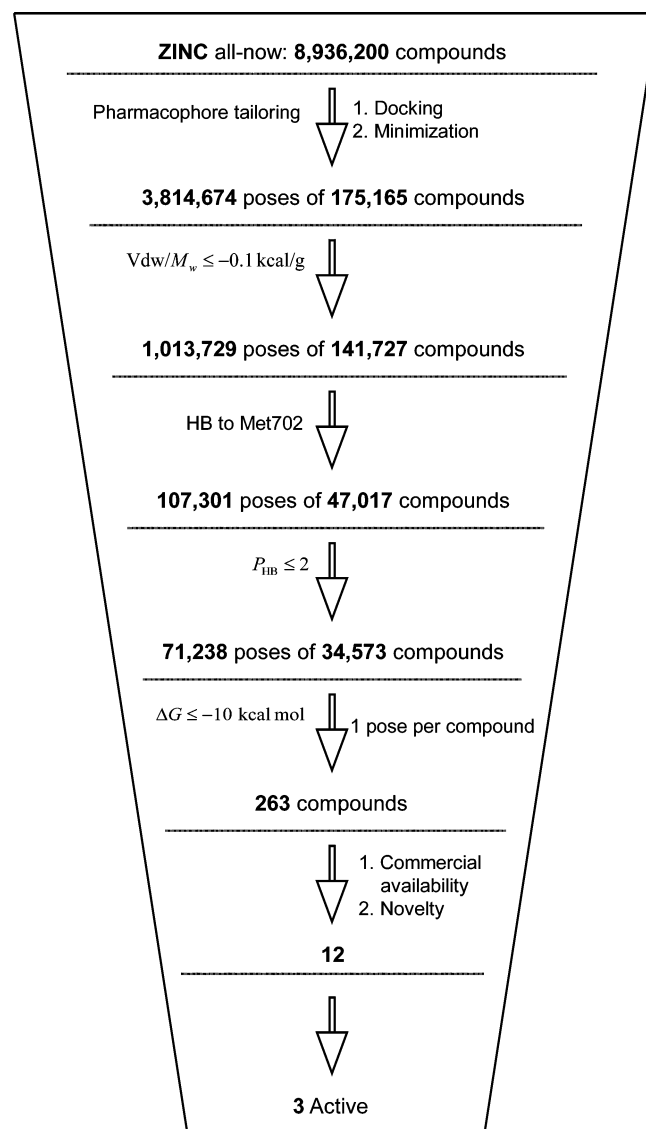
Figure 4. Schematic illustration of the high-throughput virtual screening process. The pharmacophore tailoring required 6 h, while the docking, minimization and evaluation of ΔG of binding were carried out on a computer cluster of 300 cores within one week, which corresponds to approximately 1500 days, 300 days and 150 days, respectively, of the equivalent of a single commodity processor.

Structure-based flexible ligand docking

The docking of 175 165 compounds by AutoDock yielded about 3.8 millions poses. To improve computational efficiency, three filters were applied to these poses, with focus on three complementary aspects: potency, binding specificity, and hydrogen-bonding conditions of polar atoms (Figure 4). The van der Waals efficiency of −0.1 kcal g^{-1}[23] was used as the first filter. Secondly, as the majority of kinase inhibitors are hinge binders, the hydrogen bond with the NH group of Met702 was used as the second filter to gain binding specificity, which

is most efficient among the applied filters. Lastly, a hydrogen-bonding penalty[21] of two was used to remove poses that have polar atoms buried in hydrophobic sites. With these three filters, the number of poses was reduced to about 71 000 of 35 000 compounds. Finally, the previously reported scoring function[21] was applied with a cutoff value of −10 kcal mol⁻¹, which yielded 263 compounds for further evaluation (Figure 4).

Evaluation of screening results

Interestingly, among the top 263 compounds, 55 (21%) are known type II inhibitors of 10 different scaffolds, primarily targeting Braf, Met, VEGFR, Abl1, SRC, Tie-2 and Eph (Table 1).[16,24–34] Kinase inhibitors, including type II, typically exhibit cross activity on a subfamily, as observed experimentally.[35] Indeed, some of the known inhibitors in the top 263 compounds are reported to show low micromolar to nanomolar activity on EphA3.[16,17] The successful recovery of structurally diversified known type II scaffolds out of millions of compounds indicates that the use of an MD-IF structure is very effective. Notably, none of the above compounds can be docked

as type II into the original X-ray structure without clashes with the G-loop, providing further evidence for the usefulness of inducing a generalized binding site by MD-based sampling.

In vitro validation

Twelve compounds were further selected for experimental validation, based on their novelty and commercial availability. Binding affinity was measured by a phage-display-based competition assay[17] (see Experimental Section). Three of the twelve compounds (piperazine derivatives **5**, **6** and **8**; Table 2) showed micromolar activity against phosphorylated EphA3. Unfortunately, it is not possible to carry out the same assay on unphosphorylated EphA3 due to a lack of commercial availability. It has been suggested that differential binding to phosphorylated and unphosphorylated forms of Abl1 can functionally differentiate compounds that prefer an inactive DFG-out kinase conformation (type II inhibitors) from those that do not (type I inhibitors), even for compounds that are not primarily Abl1 inhibitors but exhibit modest affinity for Abl1.[36] Interestingly, piperazine derivatives **5**, **6**, and **8** are active on unphosphorylated Abl1 (Table 2) and inactive on phosphorylated Abl1 (Table S1), which provides further evidence that they are type II inhibitors.

The nitro group of these compounds is not predicted to be involved in binding (Figure 5 a) and so could be neglected for hit optimization. Compound **5** was used as the query scaffold for a similarity search that yielded a set of 20 derivatives in the Enamine library. Four of these 20 derivatives (compounds **7** and **9–11**) show micromolar affinity for unphosphorylated Abl1 (Table 2).

Binding to the T315I Abl1 mutant

In the predicted binding mode obtained by docking and validated by MD (see below), the piperazine group of compound **5** is away from the gatekeeper Thr 699 (Figure 5 a). Automatic structural alignment of the EphA3 MD-IF structure to the complex of Abl1 with the type II inhibitor DCC-2036 (PDB: 3QRJ[2]) shows that the hydrogen bonding donors and accept-

Table 1. Representative structures of previously reported type II inhibitors identified by virtual screening of the ZINC library using the MD-IF structure of EphA3 for docking.

Core structure	Primary target	Core structure	Primary target
	Braf[24–26]		c-Met VEGFR2[27]
	VEGFR2[28]		Abl1 SRC[29]
	VEGFR PDGFR[30]		Met[31]
	c-Met[32]		Braf VEGFR[33]
	Tie-2[34]		Similar to type II inhibitors of EphA3[16]
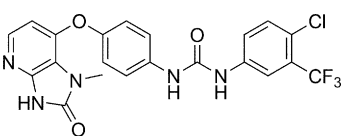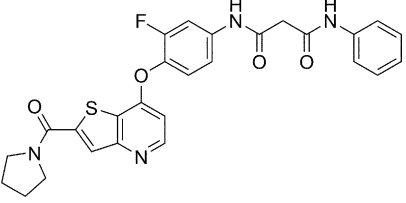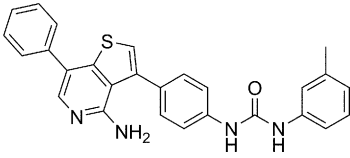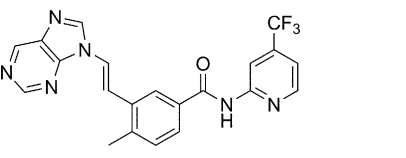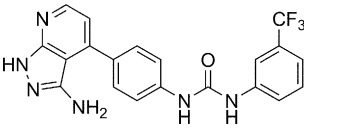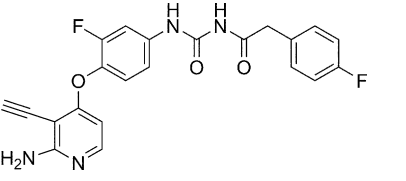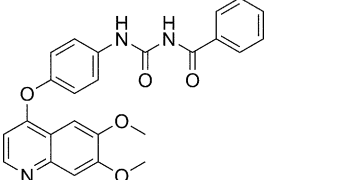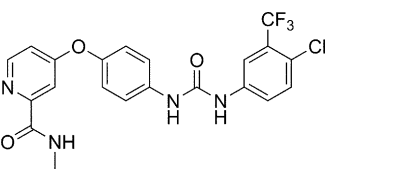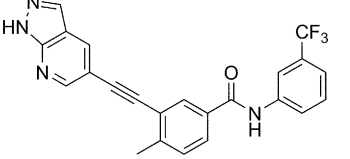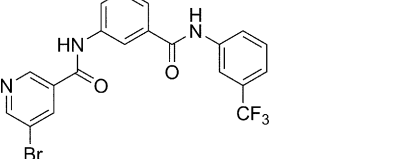
Table 2. Affinities (%) of compounds **5–11** for wild-type and mutant tyrosine kinases measured by phage-display-based competition binding assay.[a]

Compd		Substituents		EphA3	Abl1-unphosph	
		3	4	wild type	wild type	T315I
5		Cl	OCHF$_2$	53	12 (8.5 μM)[c]	45
6		Br	H	63	48	>65
7		Cl	CH$_3$	61	48	>65
8[b]		CF$_3$	H	>65	2.8 (3.9 μM)[c]	5.8
9[b]		Cl	OCH$_3$	>65	28	>65
10[b]		Cl	F	>65	38	>65
11[b]		Cl	H	60	21	55

[a] Percentage of kinase not displaced by the test compounds at 30 μM concentration with small values indicating high affinity.[17] Compounds **5**, **6**, and **8** were identified by high-throughput flexible ligand docking into the MD-IF conformation of the EphA3 receptor tyrosine kinase. Compounds **7** and **9–11** were identified by similarity search using the scaffold of compound **5**. [b] The indicated compounds are racemic mixtures, purity was checked by in-house ESI-MS and then compounds were used as purchased. [c] The K_d value in parentheses is the mean of two dose–response measurements of 11 points each.

the notable T315I gatekeeper mutant of Abl1,[2] we speculate that compound **5** might also bind to this mutant, which is the predominant mechanism of drug-induced resistance in imatinib-treated patients. Indeed, in the competition binding assay,[17] compound **8** at 30 μM shows a percent control (%ctrl) value of 5.8% on unphosphorylated T315I Abl1, which is very close to the value of 2.8% on unphosphorylated wild-type Abl1 (Table 2).

Validation of binding mode by MD simulations

To provide further evidence of the binding mode of compound **5**, two explicit solvent MD simulations were performed, starting from the complex with the MD-

ors, as well as the rings of compound **5**, are positioned and oriented in a similar way (Figure 5b). The piperazine group of compound **5** is a little further away from the gatekeeper residue Ile 315 than the phenyl ring of DCC-2036 in structure 3QRJ. Since the affinity of DCC-2036 is only slightly affected by

IF structure as obtained by docking (Figure 6; see also Figure S3 in the Supporting Information). Moreover, two MD runs were started from the X-ray structure of the complex between compound **1** and EphA3 (PDB: 3DZQ) as a basis for comparison. Overall, the binding modes of both compounds are stable
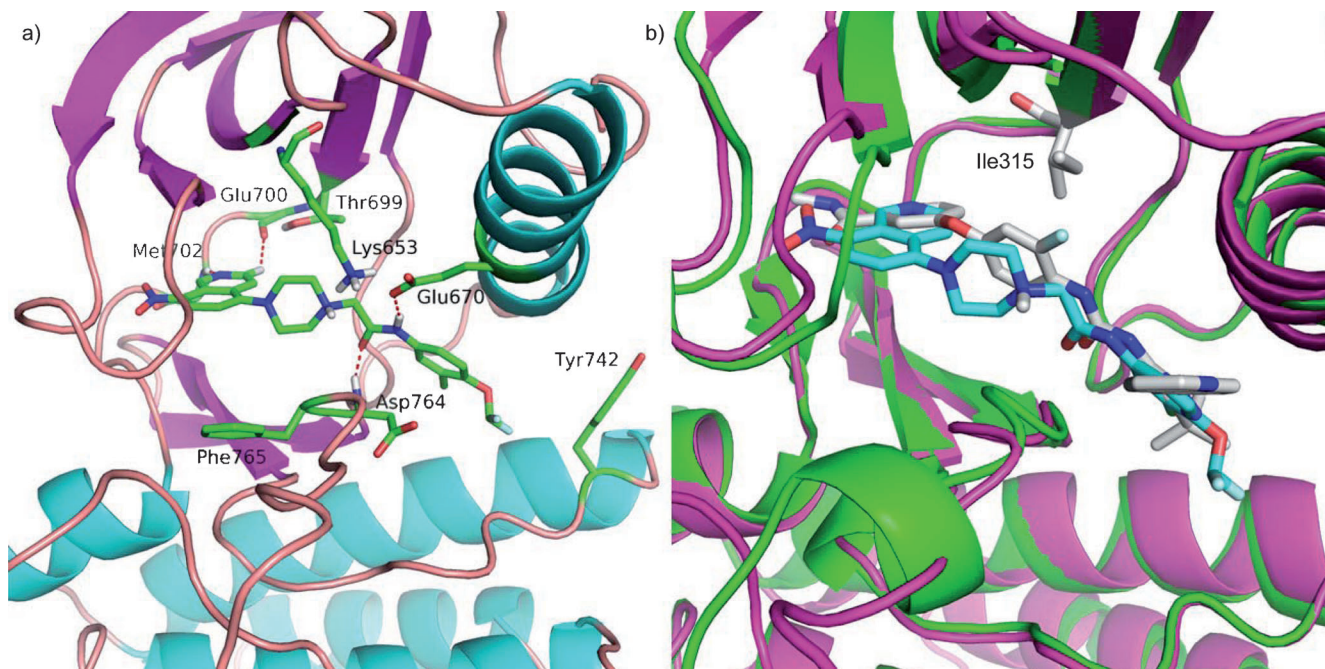
Figure 5. Predicted binding mode of compound **5** in the MD-IF structure of a) EphA3 and b) in the Abl1 crystal structure. a) Compound **5** and the EphA3 side chains involved in binding are shown by atom type coloring with carbon atoms in green, nitrogen atoms in blue, and oxygen atoms in red. b) The binding mode of compound **5** (carbon atoms in cyan) in Abl1 is obtained by structural superposition of the C$_\alpha$ atoms of the MD-IF EphA3 structure (magenta) into the crystal structure (PDB: 3QRJ) of Abl1 (green) in complex with the "switch control" inhibitor DCC-2036[2] (carbon atoms in gray). The superposition suggests that a decrease in affinity for the T315I mutant of Abl1 would not occur because there are no contacts between compound **5** and the Ile 315 side chain.

(Figure S5 in the Supporting Information). The hydrogen bond between compound **1** and the hinge is broken in one of the two MD runs, which is probably due to the electrostatic repulsion between the isoxazole oxygen and the carbonyl oxygen of Glu 700. In contrast, the two polar interactions of compound **5** with the hinge, the hydrogen bond to the NH of Met 702 and CH···O=C bond involving the carbonyl of Glu 700 (d1 and d2 in Figure 6; see also Figure S3 in the Supporting Information), are stable in both 300 ns MD simulations except for some transient ruptures. Both compounds are predicted to form stable hydrogen bonds with the DFG motif (d3 and d4; Figure 6), while the hydrogen bond between the amide NH of compound **1** or **5** and the carboxylic group of Glu 670 (d5) fluctuates strongly because the latter is solvent exposed. For this reason, the hydrogen bond to Glu 670 was not used as a pharmacophore to prefilter the ZINC library, although it is frequently observed with type II inhibitors. Nevertheless, the Glu 670 fluctuations are smaller for compound **5** than **1**, which is probably due to the favorable electrostatic interactions with the positively charged piperazine ring of compound **5**.

Conclusions

To obtain an inactive DFG-out conformation for high-throughput docking, we have run an explicit solvent MD simulation of the EphA3 receptor tyrosine kinase with a type II inhibitor placed manually in the ATP binding site upon removal of the original inhibitor of the crystal structure. Along the MD trajectory, a snapshot that accommodates four previously reported type II inhibitors was selected for high-throughput flexible ligand docking. The docked library consisted of about 175 000 compounds derived from nearly 9 million molecules using two-dimensional chemical descriptors and three-dimensional geometric constraints (i.e., relative distance and orientation of
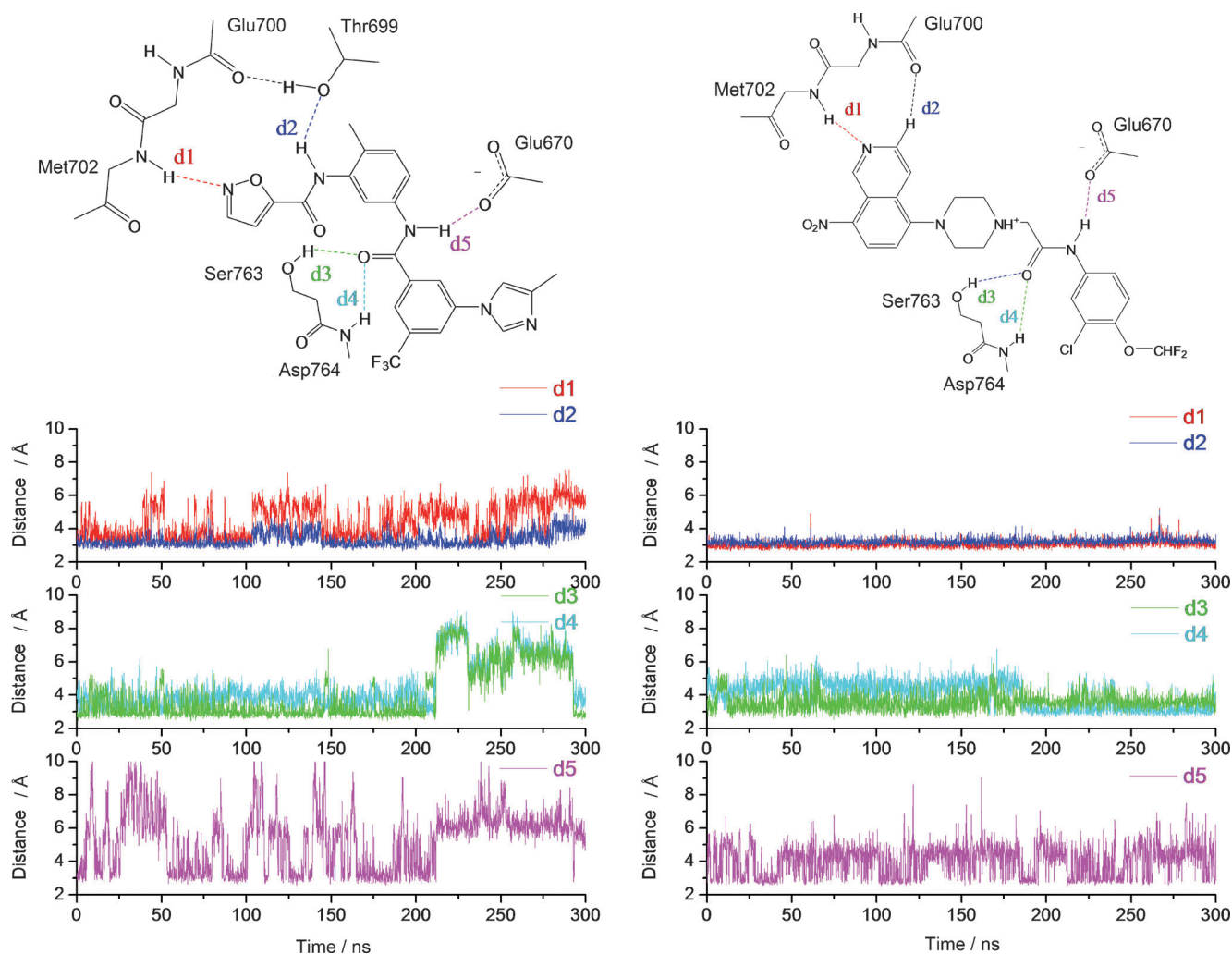
Figure 6. Explicit solvent MD validation of binding mode of compound **5**. (Left) MD run started from the X-ray structure of the complex between EphA3 and inhibitor **1** (PDB: 3DZQ). (Right) MD run started from the docked pose of compound **5** into the MD-IF structure of EphA3. (Top) Two-dimensional illustrations; (Bottom) time evolutions of hydrogen bonding distances measured between donor (or isoquinoline C$_3$ atom of compound **5**) and acceptor atoms. In the simulation with inhibitor **1**, the amide group associated with d3, d4 and d5 flipped by 180° at about 230 ns (see Figure S4 in the Supporting Information) and flipped back at 290 ns. The d5 distance shows large oscillation because of fluctuation of the Glu 670 side chain. Note also that values around 5 Å reflect single water bridged hydrogen bonds with Glu 670. Another MD run for each of compounds **1** and **5** is shown in Figure S3 in the Supporting Information. Detailed analysis is shown in Figures S4 and S5 in the Supporting Information.

pairs of functional groups). Using this procedure, we have identified a series of 5-(piperazine-1-yl)isoquinoline derivatives that exhibited low micromolar affinities for unphosphorylated Abl1 in a competition binding assay.

The following experimental evidence and computational results support the binding mode, which is predicted to be of type II: 1) The discovered scaffold shows a higher affinity for inactive than active Abl1 tyrosine kinase, a typical feature of type II inhibitors;[36] 2) the docking pose suggests a similar affinity for the gatekeeper mutant T315I as for wild-type Abl1, which was verified experimentally; 3) the hydrogen-bonding pattern and overall binding mode are preserved in two 300 ns MD simulations, started from the pose obtained by docking.

In conclusion, we have discovered a novel chemical class of type II tyrosine kinase inhibitors by using an in silico procedure based on a combination of explicit water MD simulations and high-throughput docking.

Experimental Section

Computational methods

MD simulations: The coordinates of missing atoms in the EphA3 crystal structure (PDB: 3DZQ), especially the long activation loop, were generated by the program Modeller (version 9.0).[37] To reproduce physiological pH conditions, the side chains of aspartates and glutamates were negatively charged, those of lysine and arginine residues were positively charged, while all other residues were considered neutral. The MD simulations were performed with the program NAMD (version 2.7)[38] using the all-atom CHARMM PARAM27 force field,[39] the TIP3P model of water,[40] and the CHARMM general force field for small molecules.[41]

The protein–ligand complexes were inserted into a cubic water box, with a minimal distance of 12 Å between any solute atom and the boundary of the box. Chloride and sodium ions were added to neutralize the system and to give an approximate salt concentration of 150 mM. If the distance between the water oxygen and any atom of the complex or any ion was smaller than 2.4 Å, the water molecules overlapping with the solute atoms or the ions were removed. Periodic boundary conditions were applied to avoid finite-size effects. Electrostatic interactions were calculated within a cutoff of 10 Å, while long-range electrostatic effects were taken into account by the particle mesh Ewald summation method.[42] Van der Waals interactions were treated with the use of a switch function starting at 8 Å and turning off at 10 Å. The temperature was kept constant at 310 K by using the Langevin temperature control with a damping coefficient of 1 ps^{-1}, while the pressure was held constant at 1 atm by applying a pressure piston. Before the production runs, water molecules and ions were subjected to energy minimization for 6000 steps, and a 1 ns equilibration with harmonic constraints (1 kcal mol^{-1} Å^{-2}) applied to the positions of protein C$_\alpha$ atoms excluding the G- and A-loop (residues 628–634 and 768–788, respectively). Covalent bonds involving hydrogen atoms were constrained by means of the SHAKE algorithm, and the dynamics were integrated with a time step of 2 fs.

Compound library: The compounds were downloaded from ZINC all-now library.[43] The library was firstly filtered by physicochemical properties, such as, number of donors and acceptors, molecular weight, and number of rings, according to the pharmacophores defined in Figure 3. Preparation included the assignment of

CHARMm atom types, force field parameters,[44] and partial charges,[45] and energy minimization with a distance dependent dielectric function using the program CHARMM.[46,47] Finally, the pharmacophore software LIBO version 1.0 (Zhao and Calfisch, unpublished) developed in-house was used to filter the library by pharmacophore constraints according to Figure 3.

Docking: AutoDock (version 4.0)[48] was used to generate the binding poses over the conformational search space using the Lamarckian genetic algorithm. The binding site was determined by 4.0 Å away from any atom of compound **1** in the EphA3 MD-IF structure. The number of energy evaluations was 1 750 000, and the number of poses was 30. Poses were clustered using all atom RMSD cutoff of 1.0 Å to remove redundancy. All other parameters were set as default.

Scoring function: Poses were further minimized by CHARMM in the rigid protein, and then sequentially filtered by three filters as defined in Figure 4. A previously reported scoring function was employed for ranking. It incorporates the hydrogen bonding penalty upon ligand binding, and uses the finite-difference Poisson approach to calculate electrostatic solvation.[21]

Biology

Phage-display-based binding assay: Experiments were performed at Ambit Biosciences Inc. (San Diego, USA) using binding assays as previously described.[17] Briefly, kinases were expressed as fusion proteins to T7 phage. T7-Kinase-tagged phage strains were mixed with known kinase inhibitors immobilized on streptavidin-coated magnetic beads and with test compounds. Test compounds that bind to the kinase ATP site displace the immobilized ligand from the kinase/phage, which is detected using quantitative polymerase chain reaction (PCR). The results are reported as the percentage of kinase/phage remaining bound to the ligand/beads, relative to a control (DMSO lacking a test compound). A small percent control (%ctrl) value indicates strong binding.

[1] O. Fedorov, S. Muller, S. Knapp, *Nat. Chem. Biol.* **2010**, *6*, 166–169.

[2] W. W. Chan, S. C. Wise, M. D. Kaufman, Y. M. Ahn, C. L. Ensinger, T. Haack, M. M. Hood, J. Jones, J. W. Lord, W. P. Lu, D. Miller, W. C. Patt, B. D. Smith, P. A. Petillo, T. J. Rutkoski, H. Telikepalli, L. Vogeti, T. Yao, L. Chun, R. Clark, P. Evangelista, L. C. Gavrilescu, K. Lazarides, V. M. Zaleskas, L. J. Stewart, R. A. Van Etten, D. L. Flynn, *Cancer Cell* **2011**, *19*, 556–568.

[3] A. Dixit, L. Yi, R. Gowthaman, A. Torkamani, N. J. Schork, G. M. Verkhivker, *PLoS One* **2009**, *4*, e7485.

[4] R. H. Adams, *Semin. Cell Dev. Biol.* **2002**, *13*, 55–60.

[5] R. Noberini, I. Lamberto, E. B. Pasquale, *Semin. Cell Dev. Biol.* **2012**, *23*, 51–57.

[6] G. Martiny-Baron, P. Holzer, E. Billy, C. Schnell, J. Brueggen, M. Ferretti, N. Schmiedeberg, J. M. Wood, P. Furet, P. Imbach, *Angiogenesis* **2010**, *13*, 259–267.

[7] S. A. Mitchell, M. D. Danca, P. A. Blomgren, J. W. Darrow, K. S. Currie, J. E. Kropf, S. H. Lee, S. L. Gallion, J. M. Xiong, D. A. Pippin, R. W. DeSimone, D. R. Brittelli, D. C. Eustice, A. Bourret, M. Hill-Drzewi, P. M. Maciejewski, L. L. Elkin, *Bioorg. Med. Chem. Lett.* **2009**, *19*, 6991–6995.

[8] Y. Liu, N. S. Gray, *Nat. Chem. Biol.* **2006**, *2*, 358–364.

[9] M. E. Noble, J. A. Endicott, L. N. Johnson, *Science* **2004**, *303*, 1800–1805.

[10] J. J. Liao, *J. Med. Chem.* **2007**, *50*, 409–424.

[11] F. Zuccotto, E. Ardini, E. Casale, M. Angiolini, *J. Med. Chem.* **2010**, *53*, 2681–2694.

[12] I. Kufareva, R. Abagyan, *J. Med. Chem.* **2008**, *51*, 7921–7932.

[13] M. Xu, L. Yu, B. Wan, Q. Huang, *PLoS One* **2011**, *6*, e22644.

[14] B. Nagar, W. G. Bornmann, P. Pellicena, T. Schindler, D. R. Veach, W. T. Miller, B. Clarkson, J. Kuriyan, *Cancer Res.* **2002**, *62*, 4236–4243.

[15] P. Bamborough, M. J. Brown, J. A. Christopher, C. W. Chung, G. W. Mellor, *J. Med. Chem.* **2011**, *54*, 5131–5143.

[16] Y. Choi, F. Syeda, J. R. Walker, P. J. Finerty, Jr., D. Cuerrier, A. Wojciechowski, Q. Liu, S. Dhe-Paganon, N. S. Gray, *Bioorg. Med. Chem. Lett.* **2009**, *19*, 4467–4470.

[17] M. W. Karaman, S. Herrgard, D. K. Treiber, P. Gallant, C. E. Atteridge, B. T. Campbell, K. W. Chan, P. Ciceri, M. I. Davis, P. T. Edeen, R. Faraoni, M. Floyd, J. P. Hunt, D. J. Lockhart, Z. V. Milanov, M. J. Morrison, G. Pallares, H. K. Patel, S. Pritchard, L. M. Wodicka, P. P. Zarrinkar, *Nat. Biotechnol.* **2008**, *26*, 127–132.

[18] T. L. Davis, J. R. Walker, P. Loppnau, C. Butler-Cole, A. Allali-Hassani, S. Dhe-Paganon, *Structure* **2008**, *16*, 873–884.

[19] C. J. A. Farenc, L. Hameetman, W. Zoutman, C. P. Tensen, G. Siegal, *FEBS Lett.* **2011**, *585*, 3593–3599.

[20] D. Huang, A. Caflisch, *PLoS Comput. Biol.* **2011**, *7*, e1002002.

[21] H. Zhao, D. Huang, *PLoS One* **2011**, *6*, e19923.

[22] P. Schmidtke, F. J. Luque, J. B. Murray, X. Barril, *J. Am. Chem. Soc.* **2011**, *133*, 18903–18910.

[23] P. Kolb, D. Huang, F. Dey, A. Caflisch, *J. Med. Chem.* **2008**, *51*, 1179–1188.

[24] D. Ménard, I. Niculescu-Duvaz, H. P. Dijkstra, D. Niculescu-Duvaz, B. M. Suijkerbuijk, A. Zambon, A. Nourry, E. Roman, L. Davies, H. A. Manne, F. Friedlos, R. Kirk, S. Whittaker, A. Gill, R. D. Taylor, R. Marais, C. J. Springer, *J. Med. Chem.* **2009**, *52*, 3881–3891.

[25] D. Niculescu-Duvaz, C. Gaulon, H. P. Dijkstra, I. Niculescu-Duvaz, A. Zambon, D. Menard, B. M. Suijkerbuijk, A. Nourry, L. Davies, H. Manne, F. Friedlos, L. Ogilvie, D. Hedley, S. Whittaker, R. Kirk, A. Gill, R. D. Taylor, F. I. Raynaud, J. Moreno-Farre, R. Marais, C. J. Springer, *J. Med. Chem.* **2009**, *52*, 2255–2264.

[26] B. M. Suijkerbuijk, I. Niculescu-Duvaz, C. Gaulon, H. P. Dijkstra, D. Niculescu-Duvaz, D. Menard, A. Zambon, A. Nourry, L. Davies, H. A. Manne, F. Friedlos, L. M. Ogilvie, D. Hedley, F. Lopes, N. P. Preece, J. Moreno-Farre, F. I. Raynaud, R. Kirk, S. Whittaker, R. Marais, C. J. Springer, *J. Med. Chem.* **2010**, *53*, 2741–2756.

[27] O. Saavedra, S. Claridge, L. Zhan, F. Raeppel, M. C. Granger, S. Raeppel, M. Mannion, F. Gaudette, N. Zhou, L. Isakovic, N. Bernstein, R. Deziel, H. Nguyen, N. Beaulieu, C. Beaulieu, I. Dupont, J. Wang, A. R. Macleod, J. M. Besterman, A. Vaisburg, *Bioorg. Med. Chem. Lett.* **2009**, *19*, 6836–6839.

[28] H. R. Heyman, R. R. Frey, P. F. Bousquet, G. A. Cunha, M. D. Moskey, A. A. Ahmed, N. B. Soni, P. A. Marcotte, L. J. Pease, K. B. Glaser, M. Yates, J. J. Bouska, D. H. Albert, C. L. Black-Schaefer, P. J. Dandliker, K. D. Stewart, P. Rafferty, S. K. Davidsen, M. R. Michaelides, M. L. Curtin, *Bioorg. Med. Chem. Lett.* **2007**, *17*, 1246–1249.

[29] W. S. Huang, X. Zhu, Y. Wang, M. Azam, D. Wen, R. Sundaramoorthi, R. M. Thomas, S. Liu, G. Banda, S. P. Lentini, S. Das, Q. Xu, J. Keats, F. Wang, S. Wardwell, Y. Ning, J. T. Snodgrass, M. I. Broudy, K. Russian, G. Q. Daley, J. Iuliucci, D. C. Dalgarno, T. Clackson, T. K. Sawyer, W. C. Shakespeare, *J. Med. Chem.* **2009**, *52*, 4743–4756.

[30] Y. Dai, K. Hartandi, N. B. Soni, L. J. Pease, D. R. Reuter, A. M. Olson, D. J. Osterling, S. Z. Doktor, D. H. Albert, J. J. Bouska, K. B. Glaser, P. A. Marcotte, K. D. Stewart, S. K. Davidsen, M. R. Michaelides, *Bioorg. Med. Chem. Lett.* **2008**, *18*, 386–390.

[31] Z. W. Cai, D. Wei, G. M. Schroeder, L. A. Cornelius, K. Kim, X. T. Chen, R. J. Schmidt, D. K. Williams, J. S. Tokarski, Y. An, J. S. Sack, V. Manne, A. Kamath, Y. Zhang, P. Marathe, J. T. Hunt, L. J. Lombardo, J. Fargnoli, R. M. Borzilleri, *Bioorg. Med. Chem. Lett.* **2008**, *18*, 3224–3229.

[32] P. P. Kung, L. Funk, J. Meng, G. Alton, E. Padrique, B. Mroczkowski, *Eur. J. Med. Chem.* **2008**, *43*, 1321–1329.

[33] U. R. Khire, D. Bankston, J. Barbosa, D. R. Brittelli, Y. Caringal, R. Carlson, J. Dumas, T. Gane, S. L. Heald, B. Hibner, J. S. Johnson, M. E. Katz, N. Kennure, J. Kingery-Wood, W. Lee, X. G. Liu, T. B. Lowinger, I. McAlexander, M. K. Monahan, R. Natero, J. Renick, B. Riedl, H. Rong, R. N. Sibley, R. A. Smith, D. Wolanin, *Bioorg. Med. Chem. Lett.* **2004**, *14*, 783–786.

[34] V. J. Cee, B. K. Albrecht, S. Geuns-Meyer, P. Hughes, S. Bellon, J. Bready, S. Caenepeel, S. C. Chaffee, A. Coxon, M. Emery, J. Fretland, P. Gallant, Y. Gu, B. L. Hodous, D. Hoffman, R. E. Johnson, R. Kendall, J. L. Kim, A. M. Long, D. McGowan, M. Morrison, P. R. Olivieri, V. F. Patel, A. Polverino, D. Powers, P. Rose, L. Wang, H. Zhao, *J. Med. Chem.* **2007**, *50*, 627–640.

[35] M. I. Davis, J. P. Hunt, S. Herrgard, P. Ciceri, L. M. Wodicka, G. Pallares, M. Hocker, D. K. Treiber, P. P. Zarrinkar, *Nat. Biotechnol.* **2011**, *29*, 1046–1051.

[36] L. M. Wodicka, P. Ciceri, M. I. Davis, J. P. Hunt, M. Floyd, S. Salerno, X. H. Hua, J. M. Ford, R. C. Armstrong, P. P. Zarrinkar, D. K. Treiber, *Chem. Biol.* **2010**, *17*, 1241–1249.

[37] MODELLER (copyright © 1989–2012 Andrej Sali): http://salilab.org/modeller/. A. Šali, T. L. Blundell, *J. Mol. Biol.* **1993**, *234*, 779–815.

[38] NAMD was developed by the Theoretical and Computational Biophysics Group in the Beckman Institute for Advanced Science and Technology at the University of Illinois at Urbana-Champaign (USA): http://www.ks.uiuc.edu/Research/namd/. a) J. C. Phillips, R. Braun, W. Wang, J. Gumbart, E. Tajkhorshid, E. Villa, C. Chipot, R. D. Skeel, L. Kale, K. Schulten, *J. Comp. Chem.* **2005**, *26*, 1781–1802; b) L. Kalé, R. Skeel, M. Bhandarkar, R. Brunner, A. Gursoy, N. Krawetz, J. Phillips, A. Shinozaki, K. Varadarajan, K. Schulten, *J. Comput. Phys.* **1999**, *151*, 283–312.

[39] A. D. MacKerell, Jr., D. Bashford, M. Bellott, R. L. Dunbrack, Jr., J. D. Evanseck, M. J. Field, S. Fischer, J. Gao, H. Guo, S. Ha, D. Joseph-McCarthy, L. Kuchnir, K. Kuczera, F. T. K. Lau, C. Mattos, S. Michnick, T. Ngo, D. T. Nguyen, B. Prodhom, W. E. Reiher, B. Roux, M. Schlenkrich, J. C. Smith, R. Stote, J. Straub, M. Watanabe, J. Wiorkiewicz-Kuczera, D. Yin, M. Karplus, *J. Phys. Chem. B* **1998**, *102*, 3586–3616.

[40] W. L. Jorgensen, J. Chandrasekhar, J. D. Madura, R. W. Impey, M. L. Klein, *J. Chem. Phys.* **1983**, *79*, 926–935.

[41] K. Vanommeslaeghe, E. Hatcher, C. Acharya, S. Kundu, S. Zhong, J. Shim, E. Darian, O. Guvench, P. Lopes, I. Vorobyov, A. D. Mackerell, Jr., *J. Comput. Chem.* **2010**, *31*, 671–690.

[42] T. Darden, D. York, L. Pedersen, *J. Chem. Phys.* **1993**, *98*, 10089–10092.

[43] J. J. Irwin, B. K. Shoichet, *J. Chem. Inf. Model.* **2005**, *45*, 177–182.

[44] F. A. Momany, R. Rone, *J. Comput. Chem.* **1992**, *13*, 888–900.

[45] K. T. No, J. A. Grant, H. A. Scheraga, *J. Phys. Chem.* **1990**, *94*, 4732–4739.

[46] B. R. Brooks, R. E. Bruccoleri, B. D. Olafson, D. J. States, S. Swaminathan, M. Karplus, *J. Comput. Chem.* **1983**, *4*, 187–217.

[47] B. R. Brooks, C. L. Brooks III, A. D. Mackerell, Jr., L. Nilsson, R. J. Petrella, B. Roux, Y. Won, G. Archontis, C. Bartels, S. Boresch, A. Caflisch, L. Caves, Q. Cui, A. R. Dinner, M. Feig, S. Fischer, J. Gao, M. Hodoscek, W. Im, K. Kuczera, T. Lazaridis, J. Ma, V. Ovchinnikov, E. Paci, R. W. Pastor, C. B. Post, J. Z. Pu, M. Schaefer, B. Tidor, R. M. Venable, H. L. Woodcock, X. Wu, W. Yang, D. M. York, M. Karplus, *J. Comput. Chem.* **2009**, *30*, 1545–1614.

[48] AutoDock 4.0 (http://autodock.scripps.edu/). a) D. S. Goodsell, A. J. Olson, *Proteins* **1990**, *8*, 195–202; b) G. M. Morris, D. S. Goodsell, R. S. Halliday, R. Huey, W. E. Hart, R. K. Belew, A. J. Olson, *J. Comp. Chem.* **1998**, *19*, 1639–1662.